Solid-State Lithium Ion Electrolytes

C. Tealdi, E. Quartarone and P. Mustarelli

1 Introduction

Lithium-ion batteries are mature products in portable electronics, and are considered the most promising storage systems for automotive, and even for geographical electric grids [1]. It is also accepted that the current research on lithium-ion batteries will likely generate only an incremental improvement of the performances of these storage systems, whereas any quantum jump will require a substantial change of the cell chemistry, e.g. the development of Li-air or Li-sulphur technology [2]. On the other hand, state-of-the-art Li-ion batteries are based on liquid (or gel) organic electrolytes, which pose severe problems in terms of safety and cycle life. Therefore, the replacement of the currently used organic electrolytes with inorganic solid-state electrolytes (SSEs) is very appealing. First of all, SSEs can solve several concerns on capacity losses, cycle life, operation temperatures, safety and reliability better than the liquid ones [3]. In addition, they present other advantages such as absence of leakage and pollution, and better resistance to shocks and vibrations [4]. Finally, they are generally single ion-conductors (lithium transference number equal to one), which assure maximum electrochemical efficiency and the lowering of cell over-potentials [5]. Lithium SSEs can find application in other technological sectors where all-solid-state batteries and microbatteries are often mandatory, ranging from microelectronics to sensors in medical and military fields, biomedical devices, smart cards and other micro-devices (MEMS, NEMS), and also Radio Frequency Identification (RFID) tags. This clearly justifies the increasing interest towards SSEs, as shown in Fig. 1, which reports the number of papers in this topic (taken from ISI Web of Science).

C. Tealdi · E. Quartarone · P. Mustarelli (✉)
Department of Chemistry, Section of Physical Chemistry, University of Pavia, and INSTM, Via Taramelli 12, 27100 Pavia, Italy
e-mail: piercarlo.mustarelli@unipv.it

© Springer International Publishing Switzerland 2015

Z. Zhang and S.S. Zhang (eds.), *Rechargeable Batteries*,
Green Energy and Technology, DOI 10.1007/978-3-319-15458-9_11

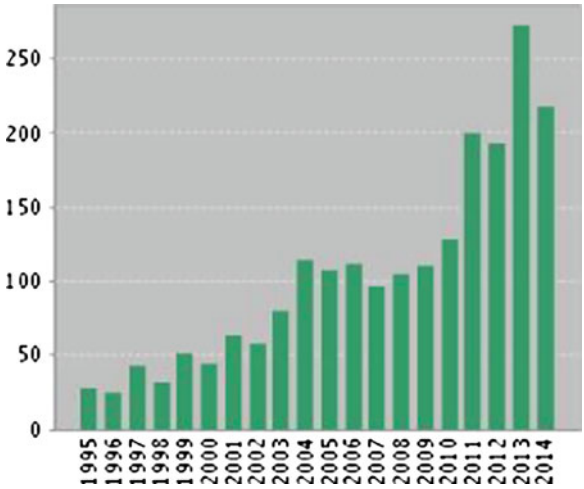

Fig. 1 Number of papers on solid-state lithium electrolytes (from ISI Web of Science, September 10, 2014)

Lithium solid-state electrolytes can be roughly divided into three main categories: (i) ceramic (CE), (ii) glasses (GL), (iii) solvent-free polymer electrolytes (SPEs). Indeed, the most appealing class is CE, which has been the object of recent good reviews [6–8]. These electrolytes can easily offer a relatively high conductivity (up to 10^{-3} Ω^{-1} cm^{-1}), and have the further advantage of a thermal expansion coefficient that can be made similar to that of ceramic electrode materials, so avoiding cracks and losses of contact during thermal cycling. An exceptionally high conductivity of 12 m Ω^{-1} cm^{-1} at room temperature was recently claimed for ceramic $Li_{10}GeP_2S_{12}$ [9], but this result has not yet been confirmed by independent research. GL electrolytes gained a great deal of attention during ’80 and ’90, chiefly because of their isotropic nature, which could allow direction-independent conductivity [10], absence of grain boundaries, ease preparation of thin films and wide attainable composition ranges [7]. At present, they are still investigated chiefly as model systems as far as concerns the relationships between local/medium range structure and transport properties [11], whereas possible technological applications are limited to anode-protective coatings for Li–O_2 batteries and electrolytes for some specific applications, e.g. in rechargeable batteries for intra-corporeal biomedical devices. In this chapter, GL electrolytes will be chiefly considered for their historical relevance. SPEs electrolytes are not generally reviewed as solid-state lithium conductors because of the polymeric—and partially amorphous—nature of the matrix [5]. On the other hand, they are practically solvent-free, and often made in form of (nano)composites with ceramic (nano)phases (SiO_2, TiO_2, layered silicates, etc.). Therefore, they will be considered in this chapter.

2 Ceramic Electrolytes

Crystalline inorganic electrolytes for Li-ion batteries can be divided into four main families of compounds, depending on their crystal structure: (1) A-site deficient perovskite-type Li-ion conductors; (2) Garnet-type Li-ion conductors; (3) NASICON-type Li-ion conductors; (4) LISICON-type Li-ion conductors.

These materials are generally prepared in bulk by solid-state reactions or sol-gel recipes. Recently, high-energy ball milling has gained interest both for inducing chemical reactivity and for particle size reduction. Thin films can be conveniently prepared by means of advanced techniques such as atomic layer deposition, whereas more conventional methods like r.f. magnetron sputtering are not well suited for these multiple-cations oxides. In the following, for each of these families we will present the main structural features, discuss the transport properties and illustrate the possible Li-ion conduction mechanism in the system.

2.1 A-Site Deficient Perovskite-Type Li-Ion Conductors

Compounds belonging to the solid solution of general formula $Li_{3x}La_{(2/3)-x}\Upsilon_{(1/3)-2x}TiO_3$ (with Υ indicating cationic vacancies on the A site) have been shown to possess a perovskite-type structure in a wide range of composition, extending approximately in the range $0.04 < x < 0.17$ [12]. Lithium ion conductivity in bulk materials of the lithium lanthanum titanate family (LLTO) was found to be extremely promising (of the order of $10^{-3}\ \Omega^{-1}\ cm^{-1}$ at room temperature), [13] largely dependent upon composition, and reaching a maximum of $1.1 \times 10^{-3}\ \Omega^{-1}\ cm^{-1}$ at room temperature for $x = 0.11$ [14]. Depending on composition and synthetic conditions, in addition to the perfectly cubic perovskite structure, tetragonal, orthorhombic and hexagonal distorted perovskite-type structures were also proposed to account for the structural features of this family. Indeed, the structural description of LLTO is still controversial, as also within a certain symmetry frequently more than one space group was proposed. Such an ambiguity mainly derives from the difficulties in identifying the Li positions, as well as the distribution of intrinsic cation vacancies. Figure 2 shows, as an example, the crystal structures of four polymorphs likely attributed to the LLTO family. As a rough guide, Li-poor compositions ($x < 0.1$) are generally reported to crystallize with orthorhombic symmetry (Fig. 2c), while for Li-rich compositions the tetragonal symmetry is preferentially reported (Fig. 2b) [15]. Both the systems are characterized by layers with large La-site occupancies, alternating with partially Li/La occupied layers characterized by a larger concentration of cationic vacancies [16]. The cubic symmetry (Fig. 2a) was obtained for specific compositions through quenching of the high temperature polymorph [17, 15 and references therein], whereas the hexagonal polymorph (Fig. 2d) was proposed for the $La_{0.5}Li_{0.5}TiO_3$ composition [18]. For a comprehensive structural survey, the reader is referred to specific review papers on the LLTO family (e.g. Ref. [4] and references therein).

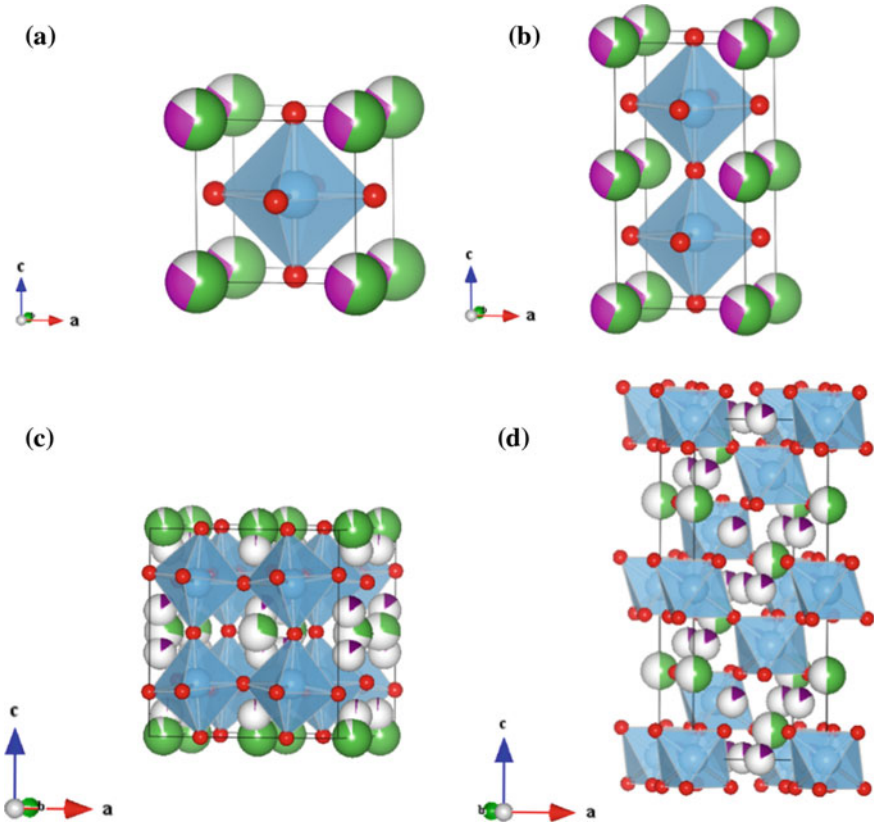

Fig. 2 Structural representation of the four main polymorphs of LLTO. **a** Cubic, space group P*m*3*m* [13]; **b** tetragonal, space group P4/*mmm* [78]; **c** orthorhombic, space group C*mmm* [79]; **d** hexagonal, space group R-3*c* [18]. Legend: *green*—lanthanum, *violet*—lithium, *pale blue*—titanium, *red*—oxygen, *grey*—cationic vacancies (Color figure online)

One important feature to note regarding the structural description of LLTO is that, for each polymorph, the crystallographic sites pertaining to La^{3+} and Li^{+} are characterized by a partial site occupancy, in addition to a certain number of vacant positions, depending on composition. The presence of such a structural disorder on the La/Li crystallographic sites and, above all, of cationic vacancies, is considered by most authors at the origin of the high conductivity values of LLTO at room temperature [17], as the most likely mechanism for Li diffusion in the system is suggested to be vacancy-mediated. A jump from a Li site into an adjacent vacant site requires that the Li ions pass through a square-type bottleneck as sketched in Fig. 3. Activation energy for Li ion migration in the system are correlated to the bottleneck size, i.e. the migration space available at the saddle point configuration.

The Arrhenius plot of conductivity for various LLTO compositions invariably shows a change in activation energy along with temperature [13, 17, 19 and references therein].

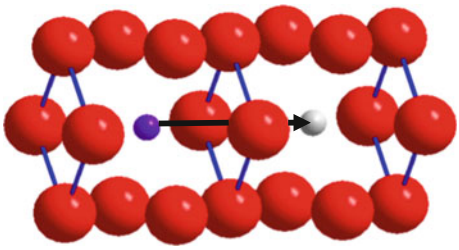

Fig. 3 Schematic representation of the square-type bottleneck for tetragonal LLTO. Ti and La ions have been omitted for clarity. Legend: *violet*—lithium, *red*—oxygen, *grey*—Li vacant site (Color figure online)

Two main regions can be identified: a low temperature region (below approximately 130 °C) following an Arrhenius-type behavior and a high temperature region where conductivity data are more correctly described by a Vogel-Tammann-Fulcher (VTF) type behavior. Such a deviation from linearity is attributed to a progressive tilting and rotation of the TiO_6 octahedra that may result in a progressive change with temperature of the available migration space for Li ion diffusion at the saddle point configuration. Activation energies for Li diffusion usually reported are around 0.3 eV, with differences due to composition and preparation methods [17]. The degree of ordering of the Li/La cations and vacancies strongly influences the transport properties of the materials, with higher conductivity generally found for the most disordered systems [20]. Interestingly, such a degree of order can be reversibly modified by careful temperature annealing in the 600–1150 °C range, thus partially allowing a modulation of the transport properties at a specific composition.

LLTO electrolytes present the advantage of being stable in dry and hydrated atmosphere and over a wide temperature range, while being characterized by a high electrochemical stability (>8 V) and almost pure ionic conductivity [16]. However, two main drawbacks affect the use of LLTO electrolytes: grain boundary resistance and electronic contribution to conductivity [7]. Grain boundary resistance can be improved through optimization of the sintering conditions, and a certain improvement of grain boundary contribution was reported in combination with the introduction of silica. Due to the presence of Ti^{4+}, LLTO is not particularly useful in combination with highly reducing negative electrodes (typically Li metal anode), as this would introduce a considerable electronic contribution to conductivity [21]. However, recent reports are showing its promising application as a separator for Li-air batteries [22].

2.2 Garnet-Type Li-Ion Conductors

Compounds exhibiting the general formula $Li_xLn_3M_2O_{12}$ (Ln = rare earth) belong to the large family of garnet-type oxides, crystallizing in a cubic structure, within

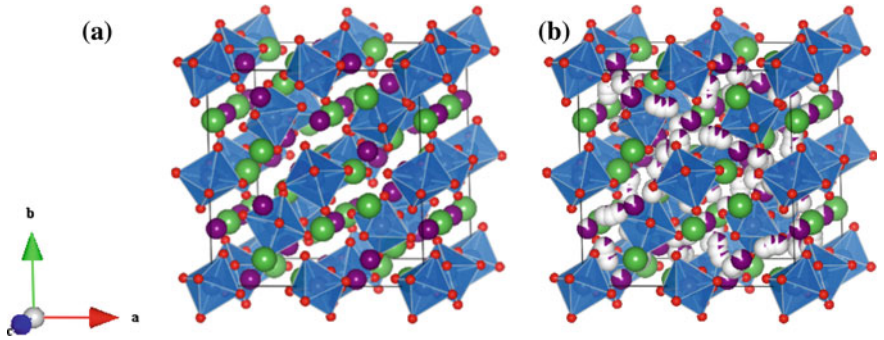

Fig. 4 Structural representation of the garnet-type structure (cubic, space group I*a-3d*) **a** stoichiometric garnet $Li_3La_3Ta_2O_{12}$; **b** Li-stuffed garnet $Li_5La_3Ta_2O_{12}$, showing the possible additional positions for Li ions and the partial site occupancy for Li ions on their respective sites [24]. Legend: *green*—lanthanum, *violet*—lithium, *blue*—tantalum, *red*—oxygen, *grey*—cationic vacancies (Color figure online)

the space group I*a-3d*, where the Ln, M and Li cations sit on distinct crystallographic sites. In particular, the Li environment is tetrahedral. When x is equal to 3, each crystallographic site is fully occupied and the compounds can be called stoichiometric garnets; when x is greater than 3, the compounds are known as Li-stuffed garnets and may exhibit high ionic conductivity [6].

The first studied Li-stuffed garnet-type compounds were $Li_5La_3M_2O_{12}$ (M = Nb, Ta) [23]. Such compounds deliver a bulk conductivity of about $10^{-6}\,\Omega^{-1}\,cm^{-1}$ at room temperature. Their crystal structure is schematically represented in Fig. 4, together with an example of the structure of stoichiometric garnet. In Li-stuffed garnets the Li ions additional with respect to the stoichiometric formula are distributed, with partial occupancy, over tetrahedral and distorted octahedral sites [24]. It is in particular the presence of vacant crystallographic sites at these additional Li positions that allows the migration of Li ions according to a vacancy-mediated hopping.

Various types of cationic isovalent and aliovalent substitutions are possible for this structure, and this allows also modulating the Li content within the system. Interestingly, an almost linear relationship between Li content and conductivity was found for $3 < x < 7$ [23, 25], although differences in transport properties may depend on both synthesis and sintering conditions. Indeed, the thermal history of the compound can affect the Li ions distribution among the additional Li crystallographic sites available for Li-stuffed garnets. The highest bulk conductivity in the family of garnet-type Li-ion conductors, of $10^{-3}\ \Omega^{-1}\ cm^{-1}$ at room temperature, was found for the $Li_{6.4}La_3Zr_{1.4}Ta_{0.6}O_{12}$ composition [23].

The garnet-type Li ion conductors generally show high ionic conductivity, wide electrochemical window and excellent stability, even in combination with metallic Li as the anode material, thanks to the low tendency of element such as Ta, Nb and Zr to change their oxidation state. This also ensures negligible electronic contributions to the conductivity.

2.3 NASICON-Type Li-Ion Conductors

Compounds of general formula $LiA_2(PO_4)_3$ (A = Ti, Zr, Ge, Hf) belong to the family of NASICON-type Li ion conductors. Most of the NASICON (Na SuperIonic CONductors) materials crystallize in a rhombohedral three-dimensional (3D) network structure (space group R-3c) characterized by large tunnels perpendicular to the *c* axis (Fig. 5a). Deviations form this symmetry were reported for lithium-excess compounds, e.g. $Li_3Ti_2(PO_4)_3$, in which two types of crystallographic sites are available for Li [26]. These two sites are partially occupied and such vacant sites represent a favourable condition to promote Li diffusion in the system (Fig. 5b). The degree of order/disorder of Li ions between the A1 and A2 sites, as well as their occupation, is dependent upon synthetic conditions and composition. Grain boundary resistance is high in polycrystalline samples but, in general, a good densification process will reduce porosity and improve Li ion conductivity [27].

Among the $LiA_2(PO_4)_3$ system, the compounds with Ti present high Li ion conductivity [7 and reference therein]. Partial substitution of Ti^{4+} by Al^{3+} results in an improved conductivity for the series $Li_{1+x}Al_xTi_{2-x}(PO_4)_3$, with the composition $Li_{1.3}Al_{0.3}Ti_{1.7}(PO_4)_3$ showing the best performances (about 3×10^{-3} Ω^{-1} cm^{-1}).

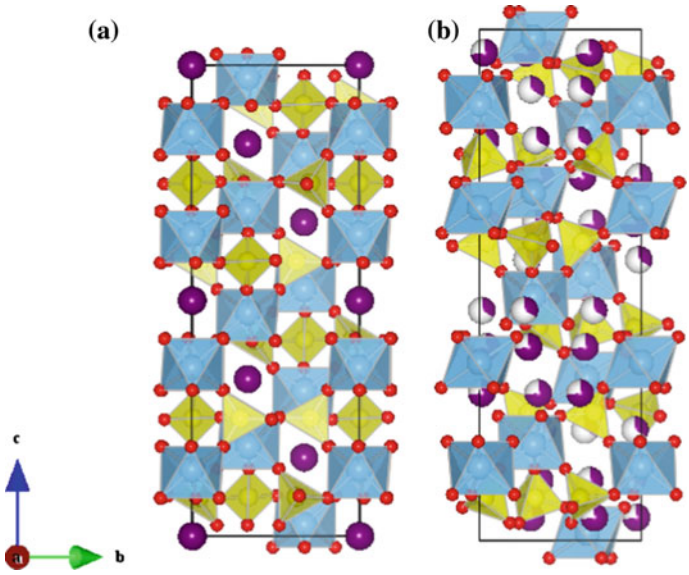

Fig. 5 Structural representation of the NASICON-type structure of **a** $LiTi_2(PO_4)_3$ (space group R-*3c*) showing the Li ions channels along the *a* axis; **b** $Li3Ti_2(PO_4)_3$ (space group R-*3*) showing the Li sites partially occupied [26]. Legend: *yellow*—phosporus, *violet*—lithium, *blue*—titanium, *red*—oxygen (Color figure online)

Just like the LLTO family of Li ion conductors, $LiTi_2(PO_4)_3$-based electrolytes are unstable towards Li metal anodes due to the facile reducibility of Ti^{4+} [21], but their excellent stability in water and air has prompted their application in all-solid-state lithium batteries as well as in lithium/air secondary batteries [28].

2.4 LISICON-Type Li-Ion Conductors

$Li_{14}ZnGe_4O_{16}$ is the main representative of the family of oxides known as LISICON (Lithium SuperIonic CONductors). The crystal structure of this family of compounds is a 3D skeleton where lithium ions can occupy four different crystallographic sites, two of them being interstitial sites where the Li ions are highly mobile. The conductivity of LISICON-type materials is generally poor, of the order of 10^{-7} Ω^{-1} cm^{-1} at room temperature, although it rapidly increases to 0.125 Ω^{-1} cm^{-1} at 300 °C [29]. Use of $Li_{14}ZnGe_4O_{16}$ is therefore impracticable because of its low conductivity at room temperature as well as its high reactivity towards Li metal.

The search for conductivity improvements in LISICON-type materials brought to the investigation of the thio-LISICON family of Li-ion conductors, in which the oxide ions are replaced by sulphur. The thio-LISICON family is represented by the general formula $Li_{4-x}A_{1-y}B_yS_4$ with A = Si, Ge and B = P, Al, Zn, Ga. The parent compound of this family is Li_4GeS_4 and its structure is based on isolated GeS_4 tetrahedra. In this structure (Fig. 6a) Li^+ ions are located in both octahedral and tetrahedral sites; LiS_6 octahedra are connected each other to form chains along the *b*-axis [30–32]. The conductivity of thio-LISICON materials exceeds 10^{-4} Ω^{-1} cm^{-1} at room temperature and is largely dependent upon composition. The highest conductivity of 2.2×10^{-3} Ω^{-1} cm^{-1} was reported for the system $Li_{3.25}Ge_{0.25}P_{0.75}S_4$, suggesting that lithium ion distribution and the presence of vacant sites on the Li sublattice compared to the parent Li_4GeS_4 compound positively affect the Li ion

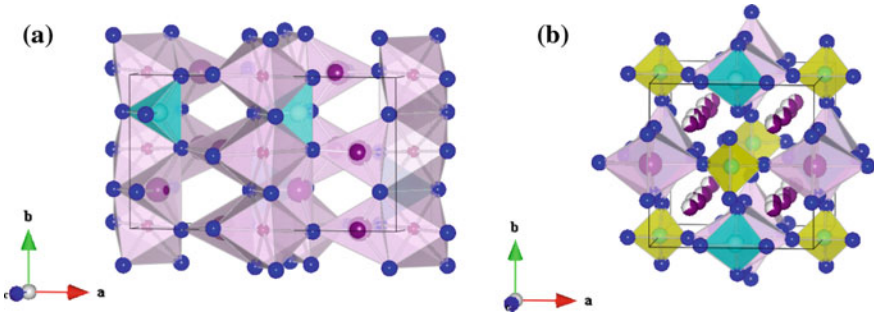

Fig. 6 **a** Crystal structure of Li_4GeS_4 [30–32]; **b** crystal structure of $Li_{10}GeP_2S_{12}$ [9] showing the channels running parallel to the *c* axis and occupied by the mobile Li ions on partially filled crystallographic sites. Legend: *yellow*—phosphorus, *cyano*—germanium, *violet*—lithium, *blue*—sulphur (Color figure online)

conduction in the structure. A similar effect was reported for the $Li_{4-x}Si_{1-x}B_xS_4$ system (B = Al, P), for which both the introduction of Li vacancies (Al doping) and Li interstitials (P doping) resulted in improved conductivities compared to Li_4SiS_4, with better performances for the Si-P solid solution.

As already stated, even higher values were claimed for the compound $Li_{10}GeP_2S_{12}$, presenting a conductivity of $1.2 \times 10^{-2}\ \Omega^{-1}\ cm^{-1}$ at room temperature [9]. $Li_{10}GeP_2S_{12}$, although closely related to the thio-LISICON family of conductor, present a completely different crystal structure (Fig. 6b) where Li ions with partial occupancy are present in channels running along the *c* crystallographic axis.

3 Glassy Electrolytes

3.1 Historical Framework

Warburg was the first one to report on ionic conduction in glasses at the beginning of the 20th century [33]. Glasses were also the first solid electrolytes to be used in thermochemical probes, and many cation-sensitive glass electrodes have been reported over the years. However, a characteristic of these glasses was their relatively high electrical resistivity at room temperature. The progresses in identifying glasses with higher ion conductivity were very slow until the '70s, probably because of the lack of studies about the local glass structure and the inability to separate carrier and mobility contributions to the conductivity.

The first examples of Fast Ion Conducting (FIC) glasses—at that time called "superionic"—were reported by Kunze in 1973 [34], and by Chiodelli et al. in 1974 [35]. Both these works were concerned with the transport of Ag^+ ions in $AgI\text{-}Ag_2MO_4$ (M = Se, Cr, W, Mo) glassy systems.

3.2 FIC Glasses Structure, Composition and Fabrication

Glasses are amorphous solids that present the glass transition, T_g, a quasi-thermodynamic phenomenon resembling a 2nd order phase transition. FIC glasses may be binary, ternary or even quaternary systems, including:

- one or two glass formers A_xB_y (A = Si, P, Ge, B; A = O, S);
- one glass modifier M_xA_y (M = Li, Na, K, Mg, Ag; A = O, S);
- one or more dopants M_xD_y (M = Li, Na, K, Mg, Ag; D = I, Cl, Br).

Here, Si, P, Ge and B are the classical glass formers individuated by Zachariasen chiefly on the basis of their ability to form coordination tetrahedra [36]. However, other metals usually forming different polyhedra (e.g. octahedra) can act as glass formers at least in certain composition ranges, e.g. MoO_2 in $AgI–Ag_2MoO_4$ [37].

Glasses were traditionally prepared by melt-quenching oxides, carbonates and/or nitrates at high temperature (even well above 1000 °C), and by pouring the melt on cold surfaces, or in liquid nitrogen. Glass-forming regions are normally reported in 2D and 3D ceramic phase diagrams. Glass-forming regions could be expanded by fast-quenching (up to 10^6 K/s) obtained by means of roller-quenchers [38]. During '90s sol-gel recipes were increasingly used to prepare silicate and later borate glasses [39]. Sol-gel techniques, in fact, allowed a further increase of the glass-forming regions and reduced the loss of light elements (e.g. Li, Na), thanks to the milder thermal conditions with respect to standard melt quenching.

During the last years, high-energy mechanical milling became a commonly used method to form amorphous materials and glasses [40]. This technique has two major advantages with respect to the other methods: the process is very simple and the synthesis can be performed at or near room temperature. Another advantage is that high-energy milling can induce chemical reactions and, therefore, make new compositions available.

3.3 Models of Ion Transport

Chandra et al. [11] recently published a thorough review on ion transport in FIC glasses. In most cases, ionic conduction is due to the motion of a single ionic species, either anion or cation. We may express the conductivity, σ, as the product of carrier charge concentration, n, and mobility, μ

$$\sigma = \mathrm{Ze}\, n\, \mu \tag{1}$$

where Ze is the charge on the conducting ion. The problem of modeling the ionic conductivity in glasses is that of understanding, and possibly separating, what determines n and μ. In the discussion of ionic conduction processes in glass, the models recurring up to the '90s were:

(i) *the strong electrolyte or Anderson-Stuart (A-S)*;
(ii) *the weak electrolyte (WE)*;
(iii) *the defect hypotheses.*

(i) The A-S model suggests that a substantial fraction of the ions is conducting. The activation energy, ΔE_A, is made of two terms

$$\Delta E_A = \Delta E_B + \Delta E_S \tag{2}$$

where ΔE_B is the electrostatic binding energy and ΔE_S is the so-called "strain energy", which accounts for the mechanical forces acting upon the ion as it

expands the structure in order to move between sites [41]. Within some approximations, the A-S model gives

$$\Delta E_B = bZZ_0e^2/g(r + r_0) \tag{3}$$

$$\Delta E_S = 4pGr_0(r - r_D)^2 \tag{4}$$

where b and g are adjustable parameters, with the latter being set equal to the dielectric permittivity. Z and r and Z_0 and r_0 are the charges and radii of cation and oxygen anion, respectively, r_D is the radius of the network constriction between the sites occupied by the cations, and G is the shear modulus of the glass.

The A-S model has been mainly applied to the borate glasses [42]. Here, ΔE_B decreases substantially with increasing alkali oxide, and this is probably due the cation jump distance, which decreases by decreasing the cation site separation, and thereby causing a greater overlapping of the coulomb orbitals.

(ii) WE theory was proposed by Ravaine and Souquet [43, 44]. They noted some similarities between the electrochemistry of glasses and aqueous systems, and hypothesized that when a modifier oxide or another dopant salt is added to a glassy matrix, alkali dissociation is the dominant energetic barrier experienced by the cation during the conduction process. Once a cation has been dissociated from its charge-compensating ion, it is free to migrate until it recombines. The dissociation takes place following simple chemical equilibria, e.g.

$$Li_2O \leftrightarrow Li^+ + OLi^- \tag{6}$$

where OLi^- is called the "dissociated anion site" and Li^+ is the "free" cation. In other words, whereas the A-S model supposes that the majority of cations do contribute to the conductivity, which is essentially determined by the mobility term, μ, the WE theory claims that only a small fraction of the ions are contributing, at a given time, to the conduction process. It should be pointed out that A-S is a "microscopic" approach, whereas WE is a "thermodynamic" one. In order to reconcile these two views, Martin and Angell [45] suggested these two models could be thought as the extremes of a more general approach, where both mobility and concentration cause conductivity variations. The two extreme models are applicable when one of the two barrier terms, migration (ΔE_S) or binding (ΔE_B), is the dominant one for a given glass: if $\Delta E_B > \Delta E_S$ the glass behaves like a weak electrolyte whereas, in contrast, the glass is a strong one. Since a strain energy barrier is always present because of the volume requirements of the migrating cations, the authors postulate the existence of metastable sites of "intermediate" energy to account for both dissociated and non-dissociated states.

(iii) Ionic transport in crystals usually involves migration of defects (vacancies, interstitial ions, interstitial pairs). Haven and Verkerk [46] argued that when the ionic motion involves defect mechanisms the experimental diffusion coefficient, D, is different (because of correlation effects) from the calculated one, D^*, which obeys the Nernst-Einstein equation

$$D^* = \sigma kT/ne^2 \tag{7}$$

Here, n is again the carrier concentration, and the other symbols have the usual meaning. The so-called "Haven ratio", D/D^*, gives information about the nature of the mechanisms involved in the conduction. In crystals the formation of defects can be treated in term of a quasi-chemical equilibrium, where concentrations and mobility of the defects may be controlled with doping. Whereas for a long time we believed that such a procedure could not be applied to glasses, since the ions cannot be considered as "foreign" to the matrix [47], Moynihan and Lesikar [48] applied the concept of doping to the Mixed Alkali Effect (the combination of two cations in a common glassy matrix, MAE), to explain the rapid falls in conductivity.

More recently, other microscopic and thermodynamic models were proposed to account for conductivity in FIC glasses. The most important of them are:

(a) *Random-site model*
Assuming that all the available ions as potentially mobile, Nassau et al. [49] proposed there should exist a wide distribution of alkali ion sites in glasses having differing local free energies. The activation energies of conductivity in these glasses will vary resembling the distribution of the local free energies. Glass and Nassau observed that the activation energy behaved as a linear function of Li content for many Li-based FICs, including Li_2O:Al_2O_3, LiO_2:B_2O_3, Li_2O:Ga_2O_3 etc.

(b) *Decoupling index model*
Angell [50] proposed the so called "decoupling index model" by introducing an index R_τ defined as the ratio of two relaxation times:

$$R_\tau = \tau_s/\tau_\sigma \tag{8}$$

where τ_s and τ_σ are the mechanical (=structure) and the electrical (=transport) relaxation times, respectively. Glasses with high R_τ values (e.g. the inorganic ones based on Zachariasen's glass formers) are termed "strong", whereas if R_τ is low they are called "fragile" (e.g. polymers and organic liquids like glycerol). For Ag^+ ion conducting iodomolybdate glasses, $R_\tau \sim 10^{14}$ [51], whereas for poorly conducting glasses, $R_\tau \sim 10^4$. Because there is such a large variation in R_τ, viscosity is indicative of analogous variations in ionic mobility and conductivity. In the lower temperature region (below the T_g), R_τ is generally higher than 10^{12}, which is indicative of the fact that the ion transport is decoupled from structural dynamics. R_τ changes very rapidly across the glass transition.

(c) *Cluster by-pass model*
Ingram et al. [52] suggested that in FIC glassy electrolytes ordered clusters (macro domains) with diameter in the range 2.5–5.0 nm will exist, within which preferred conducting pathways (a sort of connecting tissue) are imbedded. Fast ion conduction may be described as the migration of mobile ions through these preferred conducting pathways, which surround insulating (or less conducting) clusters. When the glass is quenched below T_g, the residual liquid, initially surrounding the clusters, gets solidified as a highly disordered phase forming conducting pathways. The presence of a few foreign cations on the surface of the clusters during cooling may cause blocks to preferred pathways. These blocks divert the current through the clusters. Cluster bypass model successfully provided simple explanations of transport in many FIC glasses, including those exhibiting mixed-alkali effect, high value of decoupling index, R_t, as well as the curvature observed in Arrhenius plots of some AgI-rich glasses, which was explained as a result of continuous exchange of mobile ions between cluster and tissue region [53].

(d) *Dynamic structure model (DSM)*
The approach proposed by Bunde et al. [54, 55] is based on number of key features, the most important of them being: (i) at temperatures far below the glass transition temperature, the glassy structure is completely frozen; (ii) the mobile cations themselves are active enough to create/determine their own glass structures; (iii) ion transport in glasses takes place stepwise following a jump/hop mechanism. Within this model the Authors were able to explain some important findings about FICs, and namely:

- the anomalous dependence of ionic conductivity on the content of glass modifier. Up to 6 orders-of-magnitude increase were observed in the ionic conductivity of $x\mathrm{Na_2O}:(1-x)\mathrm{B_2O_3}$ glass when x increased from 0.15 to 0.5;
- the strong decrease of the ionic conductivity as a consequence of MAE. For example, decreases of conductivity up to 10^4 times were observed in $[x\mathrm{K_2O}:(1-x)\mathrm{Li_2O}]:2\mathrm{SiO_2}$ for $x \cong 0.5$ with respect to the pure binary systems;
- other minor consequences of MAE, such as variation in diffusion coefficient of mobile cations, maxima of Haven's ratio, occurrence of internal friction peaks in the mechanical loss spectrum.

(e) *MIsmatch Generated Relaxation for the Accommodation and Transport of IONs* (*MIGRATION*) *model*
Recently, Funke and co-workers [56] explored the concept of ion hopping dynamics in disordered materials. Following their approach, structural and dynamic disorders are the key factors to understand ion conduction in FIC glasses. Here, ionic transport can no longer be described in terms of individual defects performing random walks in a static energy landscape, but rather in terms of a more challenging many-particle problem, with the mobile ions

interacting with each other and with their surrounding matrix. Each mobile ion is surrounded by its mobile neighbors, which create a cage-like potential for it. By ion initial hop, a mismatch is created and the actual position of the ion would be different from the position where it is expected for by the neighbors. According to the MIGRATION concept, the system operates in order to reduce the mismatch through two competing relaxations ways: single-particle and many-particles. In the single-particle route the ions hop backwards, whereas in the other route the neighbours rearrange themselves. The mismatch-generated relaxation process occurring along the many-particle route finally leads to an accommodation of the ion at the new site.

(f) *Graded percolation* (*GP*) *model*
This model was recently proposed by Mustarelli et al. [57] in order to describe the transport properties of AgI-based glasses. It is based on previous Reverse Monte Carlo (RMC) structural models of borate and molybdate glasses [58], coupled with bond valence calculations, which showed that the conductivity is related to the formation of "infinite pathways clusters" for transport, where the silver ions do experience a mixed iodine/oxygen (I/O) coordination. In GP model, the main factor affecting ionic conductivity is the mobility of the Ag^+ carriers, which is controlled by the Ag local environment. Ionic conductivity is explained in terms of a percolation between a low-conducting phase (purely oxygen-coordinated sites), and a high-conducting one (I/O coordinated sites). The percolation takes place along pathways (nano-channels) with fractal structure. The nature of the glass network (connectivity and dimensionality) plays a significant role only for low I/O values. This allowed explaining the transport and thermal anomalies observed in AgI-based borate and phosphate glasses.

3.4 Li-Based FIC Glasses

Lithium-ion conducting glasses can be divided into two big categories: oxides and sulphides. Lithium oxide glasses are more common and easy to prepare, however their conductivity generally does not exceed 10^{-8}–10^{-6} Ω^{-1} cm^{-1}, which is not enough for applications in high power density devices such as lithium batteries. Sulphide glasses can offer much higher conductivity levels (10^{-5}–10^{-3} Ω^{-1} cm^{-1}) due to the higher polarizability of sulphur ions, however they are very sensitive to moisture and do require inert ambient for preparation and handling. In particular, reaction with moisture can generate H_2S [21]. This problem can be partially solved, at the expenses of the conductivity level, by substituting a fraction of sulphur atoms with oxygens. From the point of view of the composition, for a better addressing of the glass forming regions, it is convenient to separately discuss binary and ternary glasses.

3.4.1 Li Binary Glasses

These are glasses of the systems $x\text{Li}_2\text{O}:(1-x)\text{M}_y\text{O}_z$ and $x\text{Li}_2\text{S}:(1-x)\text{M}_y\text{S}_z$ (M = Si, B, P, Ge, etc.). The conductivity normally increases by increasing the molar fraction, x, of the glass modifier Li_2O (Li_2S). Figures 7 and 8 report the behavior of the conductivity near the room temperature for some model lithium oxide and sulphide glassy systems, respectively.

From the data here reported it is clear that sulphide glasses display ion conductivity higher than oxide ones. It is also clear that the conductivity values strongly depend on the structure of the matrix, which is almost fully interconnected in the case of Si-based glasses, gets to be more open on B-ones and is chain-like in $0.5\text{Li}_2\text{M}:0.5\text{P}_2\text{M}_5$. A good discussion of the structure-properties relationships is reported in Ref. [10].

3.4.2 Li Ternary Glasses

Ternary systems may be obtained by adding a dopant (e.g.: LiI) to the binary glass. High conductivity levels in the range 10^{-3}–10^{-2} Ω^{-1} cm^{-1} at 300 °C were early reported for $\text{LiCl}:\text{Li}_2\text{O}:\text{B}_2\text{O}_2$ [59]. Sulphide glasses are among the best Li^+ conductors at room temperature. Figure 9 reports the room temperature conductivity for several compositions as a function of LiI content. It seems that conductivity tends to a limiting value of approximately 10^{-3} Ω^{-1} cm^{-1} as also reported for silver glasses doped with AgI [57].

Another way to improve the conductivity of glasses is to exploit the so-called "mixed anion" or "mixed former" effect, where two glass formers are mixed to give

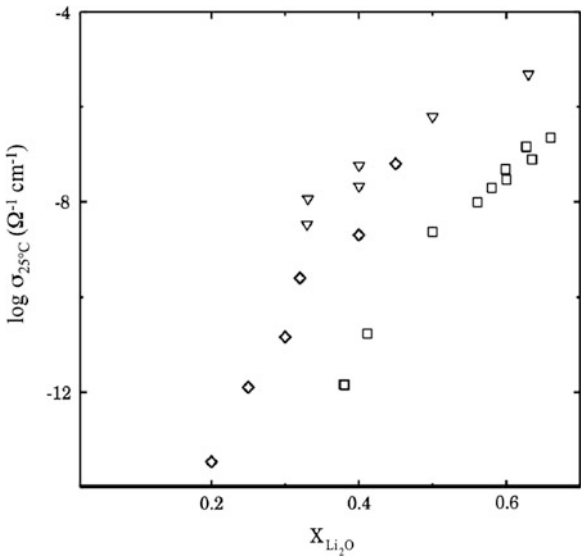

Fig. 7 Conductivity behaviour of glasses of the systems $x\text{Li}_2\text{O}:(1-x)\text{M}_y\text{O}_z$. *Triangles* $\text{Li}_2\text{O}:\text{SiO}_2$; *rhombs* $\text{Li}_2\text{O}:\text{B}_2\text{O}_3$; *squares* $\text{Li}_2\text{O}:\text{P}_2\text{O}_5$. Graph redrawn from Ref. [10] (Color figure online)

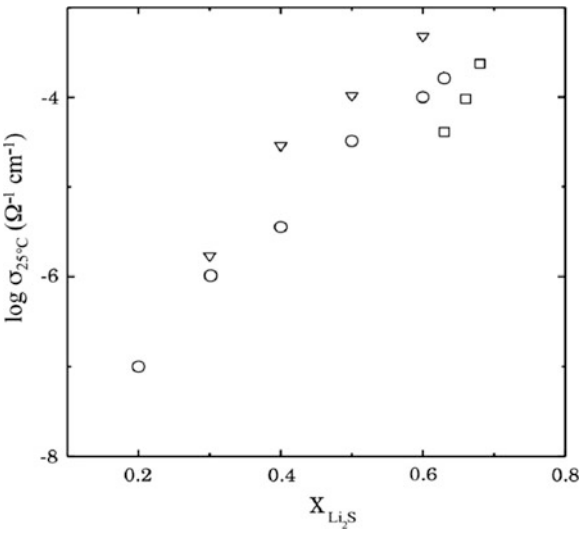

Fig. 8 Conductivity behaviour of glasses of the systems $x\mathrm{Li_2S}:(1-x)\mathrm{M_yS_z}$. *Triangles* $\mathrm{Li_2S}:\mathrm{SiS_2}$; *circles* $\mathrm{Li_2S}:\mathrm{GeS_2}$; *squares* $\mathrm{Li_2S}:\mathrm{P_2S_5}$. Graph redrawn from Ref. [10] (Color figure online)

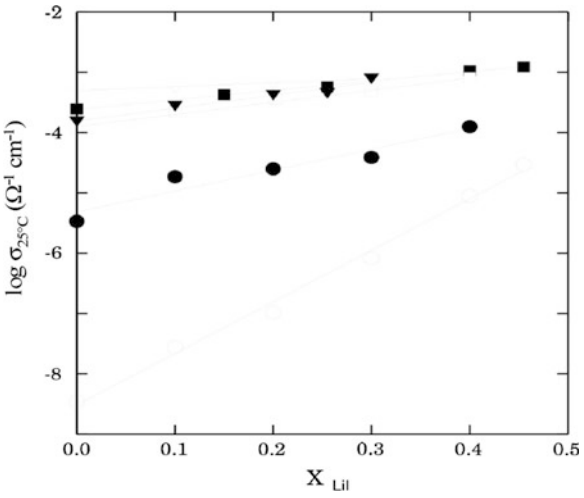

Fig. 9 Conductivity behaviour of glasses belonging to ternary systems $x\mathrm{LiI}:(1-x)[\mathrm{Li_2S}\text{-}\mathrm{M_yS_z}]$ (M = Si, P, Ge). *Triangles* $\mathrm{SiS_2}$; *circles* $\mathrm{GeS_2}$; *squares* $\mathrm{P_2S_5}$. Graph redrawn from Ref. [10] (Color figure online)

a ternary system, or even a quaternary one if a dopant is also used. Examining the alkali borophosphate families over a wide range of B/P ratios it was observed [60] that the ionic conductivity of these glasses is a complex function of composition and that, for the same alkali content, when $\mathrm{P_2O_5}$ was substituted for $\mathrm{B_2O_3}$ the conductivity passes through a maximum. The same results were later reported for sulphide glasses [61].

Among the most recent results, a conductivity value of $1.6 \times 10^{-3}\ \Omega^{-1}\ \mathrm{cm}^{-1}$ at 25 °C was reported for the glass $50\mathrm{Li_2S}:17\mathrm{P_2S_5}:33\mathrm{LiBH_4}$ [62]. Seino et al. [63] recently reported a value of $1.7 \times 10^{-2}\ \Omega^{-1}\ \mathrm{cm}^{-1}$ for the glass-ceramic composition

$70Li_2S{:}30P_2S_5$. However, the high values obtained on glass-ceramic systems are often due to grain boundary contributions and/or impurities (chiefly in the case of sulphides), and need a very careful experimental check.

4 Solid Polymer Electrolytes

With respect to ceramic and glassy materials, the polymer electrolytes show important benefits including flexibility, free-standing performances and an easier processability. In addition, the use of "dry" polymeric systems may limit some important drawbacks, related to the solvent leakage, the high Li reactivity and the consequent dendrites formation [4, 64]. They behave both as the separator and the electrolyte, also leading to more stable solid-state interfaces. In terms of battery safety, the presence of a polymer in the cell may guarantee higher thermal stability and thermal excursion up to 200 °C. Due to these promising aspects, SPEs are considered as a possible alternative to the liquid ones in Li- or Na-based batteries.

The concept of SPE dates back to 70s, when Armand firstly proposed a new ion conductor based on a lithium salt properly complexed by a polar and aprotic polymer matrix without the use of any liquid component (additives or liquid electrolytes) [65]. At the beginnings, the research on SPEs was exclusively focused on poly(ethyleneoxide) (PEO) as the complexing polymer [66]. Ever since, a lot of polymer/salt systems were deeply investigated, such as those based on PMMA, PAN, PVDF [66–69]. In principle, SPEs must satisfy some basic requirements: (i) ionic conductivity higher than 10^{-4} S/cm at room temperature, (ii) good thermal, chemical and mechanical stability, (iii) lithium transport number close to the unity, and (iv) compatibility with the electrodes and consequently wide electrochemical windows [67].

In spite of the wide spectrum of SPEs available in the literature, the preferred combinations are still those based on polyethylene oxide (PEO). PEO is a semi-crystalline polymer whose glass transition temperature T_g and melting point T_m are near −60 and 70 °C, respectively. It allows a better Li solvation due to its structural similarity to the crown-ethers and to the presence of ether oxygen in the structure, which confers some polarity ($\varepsilon_r = 8$) [4, 66–69]. Li transport takes place in the amorphous polymer domains above the glass transition temperature, T_g, via an oxygen-assisted ion hopping promoted by the long-range segmental motion along the polymer backbone (see Fig. 10).

The ionic conductivity of the PEO electrolytes, therefore, strictly depends on both crystallinity degree and T_g of the amorphous phase [70]. In particular, it is very low at room temperature ($<10^{-6}$ Ω^{-1} cm^{-1}) where the crystalline fraction of the polymer is predominant, but it abruptly increases around the melting temperature reaching 1 Ω^{-1} cm^{-1} above 80–90 °C, where the entire polymer is in a viscous liquid state. The research on SPEs ever pointed towards the enlargement of the amorphous fraction by means of several approaches. One of the most followed strategies was the choice of suitable Li salts and the identification of proper salt

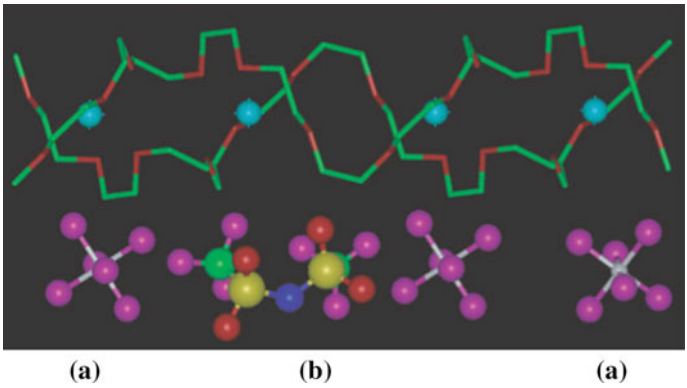

Fig. 10 Crystal structure of PEO_6:$(LiAsF_6)_{1-x}(LiTFSI)_x$. *Blue spheres* Li ions; *Pink structures* **a** AsF_6^- anion; *mixed colors structure* **b** $TFSI^-$ anion. Taken from Ref. [68] with the permission of the publisher (Color figure online)

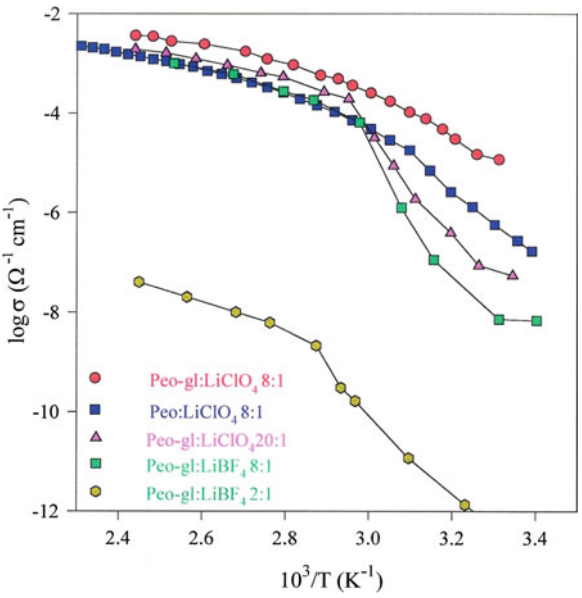

Fig. 11 Conductivity versus temperature for some PEO: LiX complexes at different molar ratio, *n*. gl: Li_2O:$3B_2O_3$ glass. Unpublished data from the Authors (Color figure online)

concentrations. Several PEO_n-LiX were explored in the past, by changing both the molar ratio *n*, expressed as mol_{EO}/mol_{Li}, and the anion X (where X = halide, ClO_4, CF_3SO_3, PF_6, TFSI, BF_4 etc.). Generally speaking, the presence of the salt increases the polymer amorphous fraction, that can reach 100 % for well-defined molar ratios, *n*, generally in the range 8–20, depending on the employed salt [4, 5]. In case of fully amorphous PEO-LiX, ionic conductivity exceeding 10^{-5} Ω^{-1} cm^{-1} is generally observed, even at room temperature (see Fig. 11).

However, the absence of crystalline domains causes a drastic worsening of the mechanical performances (dimensional stability, filmability, free-standing properties). In addition, the amorphous phase is metastable and undergoes to crystallization within days or weeks, so causing drastic drops of conductivity. At higher salt content ($n < 6$), thermal and spectroscopic techniques evidence the presence of crystalline aggregates, which are responsible for the reduction of the conductivity values, because of the formation of ion pairs. In 2005, Bruce showed that some crystalline complexes (e.g. PEO-$LiAsF_6$) with $n = 6$ are arranged in unique cylindrical structures, where the lithium ions are not coordinated by the anions. Such complexes are not good ion conductors, but their conductivity remarkably improves when the AsF_6^- anions are partially replaced by the isovalent $TSFI^-$ ones [71].

SPEs are bi-ionic systems. This means that both anions and cations are mobile; unfortunately the bulk conductivity is primarily due to the anion mobility. In fact, lithium transference numbers, t_{Li}^+, as low as 0.05–0.3 are generally obtained in case of PEO-based electrolytes [61]. The higher mobility causes an accumulation of the anions around the electrodes, because they exchanges with Li^+ only. The resulting gradients in the salt concentration are responsible for the electrode polarization and do lead to worsening of performances. Some attempts to overcome this drawback were carried out during these last decades, as for instance the use of large and heavy anions (e.g. $TFSI^-$) or of anion receptors, like boron, linear and cyclic azo-ether compounds, or calix-arene derivatives [72], which behave similarly to the crown-ethers in case of cations. However, these strategies failed for different reasons: in some cases no substantial enhancement of t_{Li}^+ was observed, in other ones the complexation of the anion caused a conductivity decrease. The more realistic strategy to forbid counter-ion diffusion is the anion anchoring to the polymer chains via chemical bonding to form single-ion conductors. The systems including charged groups along the backbone are known as polyelectrolytes [64, 73]. In the particular of case of batteries, this approach results in free cations with higher long-range mobility and consequently t_{Li}^+ values very close to unit. Several classes of polymers were investigated as matrices for single-ion conduction, ranging from organic and/or inorganic polyanions, to polymeric ionic liquids and charged di- or tri-block copolymers [73].

The technological use of PEO-salt complexes may be possible if a proper compromise among the following factors is reached: (i) suitable ionic conductivities, (ii) good mechanical properties, and (iii) higher transference number. Many efforts were made to this aim. One explored way was the blending and/or cross-linking of PEO with other compatible polymers, as poly(acrylic acid) (PAA) and poly(methylmethacrilate) (PMMA), which improve the mechanical performances and increase the conductivity as well as the lithium transport number, by blocking the anion. In particular, polystyrene has been widely used to give a better dimensional stability to the polyether systems. In this case, the physical and chemical properties of the mixed system may be modulated by changing parameters as the ratio between the two polymers [4, 73]. Gomez et al. [74] for instance, found that the ionic conductivity of poly(styrene-block-ethylene oxide) copolymers

increases with the molecular weight, due to local stresses in the block copolymer microdomains, which interfer with the capability of PEO to coordinate Li^+ cations.

The addition of ceramic particles to PEO-based electrolytes to form nano- or micro-composite systems is maybe the most interesting way to prevent the electrode degradation phenomena, to improve the chemical, thermal and mechanical stability and finally to reduce the tendency to crystallization. Many micro- and nano inorganic oxides were added to the polymer during the film casting, in particular insulating SiO_2, Al_2O_3 and TiO_2, but also superacid conducting zeolites, or lithium-based glasses, or more recently also $LiNbO_3$ or $BaTiO_3$ [75]. Besides the benefits discussed above, the fillers also improve the ionic transport and the SEI stability. The entity of these effects depends on the morphological features of the filler, namely particle dimension, which should be lower than 1 μm, and microstructure. An important advance in this field is the use of mesoporous fillers, like SBA-15 or MCM-41. It was found that the dispersion of such nanoporous fillers in PEO-$LiClO_4$ electrolytes leads to a conductivity enhancement three times higher than that obtained in case of microsized silica. This improvement has been interpreted in terms of a suppression of the PEO crystalline fraction, as proved by means of DSC measurements on the corresponding SiO_2-based composite electrolytes. The typical high surface area of the mesoporous materials favours the formation of a larger polymer/filler interphase, which has positive effect even on both electrochemical stability windows and transport numbers [75].

Some years ago, LIBOB was proposed as a new salt for PEO-based SPEs and nanocomposites with alumina and nanosized silica. This salt has a bulky anion with plasticizing properties, able to hinder the polymer crystallization. Ionic conductivity of about $10^{-5}\ \Omega^{-1}\ cm^{-1}$ were observed at 30 °C. The most interesting result was a transference number very close to 0.9 in case of a SPE based on PEO-PMMA block copolymers with high LIBOB loading (n = 3). These membranes also showed a wide electrochemical window exceeding 4.0 V and good interfacial stability with the lithium anode. A further advance in this field is the dissolution in PEO matrices of lithium borate salts, namely Li–$[CH_3(OCH_2CH_2)_nO]_3BC_3H_9$ containing a number of oxyethylene substituents, n, in the range 1–7. The salt with n = 3 shows an interesting conductivity of 2×10^{-5} S/cm at room temperature [5, 75].

Other polymers were also studied as alternative matrices for SPEs, all of them including ethylene oxide as basic unit, like for instance polyethylenoxide-methylethermethacrylate (PEOMA) and polyethylenglycol-alkylacrylate. However, no important improvements have been reported, and conductivity similar to that one observed in case of PEO-LiX complexes was typically observed [4, 73].

More recently, as a consequence of the use of ionic liquids (ILs) in lithium batteries, a new class of solid polymer electrolytes was proposed by Ohno and co. [76]. Basically, these SPEs, better known as polymeric ionic liquids (PILs), are prepared through the radical polymerization of ILs by properly combining different cations, anions and polymer backbones [77]. PILs show the potential advantage to combine the benefits of ionic liquids (high ionic conductivity, high thermal

stability, non-flammability and low volatility) with those ones of polymers, namely mechanical stability, free-standing properties, safety, easier processing, packaging, etc. However, as in the case of other polyelectrolytes, the ionic conductivity is often too low for practical applications. In fact, whereas typical conductivity values obtained with the ionic liquids are around $10^{-3}\ \Omega^{-1}\ cm^{-1}$ at room temperature, after the polymerization process the conductivity dramatically falls, sometimes even of 2–4 orders-of-magnitude. Ohno found values 10^4 times lower for the system based on ethylvinylimidazolium-TFSI after the polymerization [76]. This phenomenon was rationalized in terms of a remarkable increase of T_g and of a reduction of the free mobile ions, because of the covalent bonding of the monomer components.

Finally, the most recent promising classes in the field of SPEs are the zwitterions, identified as "Li ion dissociation enhancers", namely ionic liquids where both the anion and cation are immobilized on the same structure. If dispersed into proper PEO-like polymers, the zwitterionic compounds may increase the ionic conductivity of the polymer electrolytes [80]. In case of addition of 1-butylimidazolium-3-(n-butanesulphonate) dissociator to Lithium methylacrylate copolymers, for instance, the ionic conductivity achieves a maximum close to 0.6 m $\Omega^{-1}\ cm^{-1}$ at 30 °C, in presence of a Li^+ mole fraction in the copolymer of about 0.050.

5 Conclusions

At present, the research on solid-state Li^+ conductors is chiefly focused on ceramic materials, which seem to offer the most room for improvements. Here, in addition to the investigation of structure/transport relationships, many issues must be considered: meso- and microstructure (particle dimensions, grain boundaries, thin films, etc.), chemical, electrochemical and mechanical stability. Glasses seem to have reached their maximum potential, having been explored as far as concerns composition, transport mechanisms, local and even medium range structure. Polymers (and composite) electrolytes may reserve some good news, chiefly in terms of chemical stability towards the electrodes, and electrochemical compliance with the recently proposed 5 V cathodes.

Magistris [10] concluded his review with these words: "Composite materials, dispersed phases or dynamically heterogeneous (solid–liquid) systems are little known and have enormous potential of optimization. They usually contain at least an amorphous, or highly disordered component, and their conductivity behaviour is strongly influenced by interfacial phenomena. If our skills in controlling the fine scale morphology of the "electrolyte system" will grow enough, we may dream of imitating a natural membrane, with its switchable and highly efficient ionic channels." About twenty years later this fine control has yet to be fully realized, and a great deal of attention must be devoted to bottom-up preparation techniques, such as atomic layer deposition, pulsed laser deposition, molecular self-assembling, etc.

References

1. DOE/EPRI 2013 Electricity Storage Handbook
2. Bruce PG, Freunberger SA, Hardwick LJ, Tarascon J-M (2012) Li–O_2 and Li–S batteries with high energy storage. Nat Mater 11:19–29
3. Hayashi A, Noi K, Sakuda A, Tatsumisago M (2012) Superionic glass-ceramic electrolytes for room-temperature rechargeable sodium batteries. Nat Commun 3:856–860
4. Fergus JW (2010) Ceramic and polymeric solid electrolytes for lithium-ion batteries. J Power Sour 195:4554–4569
5. Quartarone E, Mustarelli P (2011) Electrolytes for solid-state lithium rechargeable batteries: recent advances and perspectives. Chem Soc Rev 40:2525–2540
6. Cussen EJ (2010) Structure and ionic conductivity in lithium garnets. J Mater Chem 20:5167–5173
7. Cao C, Li Z-B, Wang X-L et al (2014) Recent advances in inorganic solid electrolytes for lithium batteries. Front Energy Res 25:1–10
8. Thangadurai V, Narayanan S, Pinzaru D (2014) Garnet-type solid state fast Li ion conductors for Li batteries: critical review. Chem Soc Rev 43:4714–4727
9. Kamaya N, Homma K, Yamakawa Y et al (2011) A lithium superionic conductor. Nat Mater 10:682–686
10. Magistris A (1993) Ionic conduction in glasses. In: Scrosati B, Magistris A, Mari CM, Mariotto G (eds) Fast ion transport in solids: proceedings of the NATO advanced research workshop, Belgirate, Italy. NATO Science Series E, vol 250. Kluwer, Dordrecht, pp 120–132, 20–26 September 1992
11. Chandra A, Bhatt A, Chandra A (2013) Ion conduction in superionic glassy electrolytes: an overview. J Mater Sci Technol 29:193–208
12. Belous AG, Novitskaya GN, Polyanetskaya SV et al (1987) Study of complex oxides with the composition $La_{2/3-x}Li_{3x}TiO_3$. Inorg Mater 23:412–415
13. Inaguma Y, Chen L, Itoh M et al (1993) High ionic conductivity in lithium lanthanum titanate. Solid State Commun 86:689–693
14. Kawai H, Kuwano J (1994) Lithium ion conductivity of A-site deficient perovskite solid-solution $La_{0.67-x}Li_{3x}TiO_3$. J Electrochem Soc 141:L78–L79
15. Gao X, Fisher CAJ, Kimura T et al (2013) Lithium atom and A-site vacancy distributions in lanthanum lithium titanate. Chem Mater 25:1607–1614
16. Bohnke O (2008) The fast lithium-ion conducting oxides $Li_{3x}La_{2/3-x}TiO_3$ from fundamentals to application. Solid State Ionics 179:9–15
17. Stramare S, Thangadurai V, Weppner W (2003) Lithium lanthanum titanates: a review. Chem Mater 15:3974–3990
18. Alonso JA, Sanz J, Santamaria J et al (2000) On the location of Li^+ cations in the fast Li-cation conductor $La_{0.5}Li_{0.5}TiO_3$ perovskite. Angew Chem Int Ed 39:619–621
19. Emery J, Buzare JY, Bohnke O et al (1997) Lithium-7 NMR and ionic conductivity studies of lanthanum lithium titanate electrolytes. Solid State Ionics 99:41–51
20. Harada Y, Hirakoso Y, Kawai H et al (1999) Order-disorder of the A-site ions and lithium ion conductivity in the perovskite solid solution $La_{0.67-x}Li_{3x}TiO_3$ (x = 0.11). Solid State Ionics 121:245–251
21. Knauth P (2009) Inorganic solid Li ion conductors: an overview. Solid State Ionics 180:911–916
22. Inaguma Y, Nakashima M (2013) A rechargeable lithium-air battery using a lithium ion-conducting lanthanum lithium titanate ceramics as an electrolyte separator. J Power Sour 228:250–255
23. Thangadurai V, Kaack H, Weppner WJF (2003) Novel fast lithium ion conduction in garnet-type $Li_5La_3M_2O_{12}$ (M = Nb, Ta). J Am Ceram Soc 86:437–440
24. Cussen EJ (2006) The structure of lithium garnets: cation disorder and clustering in a new family of fast Li^+ conductors. Chem Commun 4:412–413

25. Ramzy A, Thangadurai V (2010) Tailor-made development of fast Li Ion conducting garnet-like solid electrolytes. ACS Appl Mater Interfaces 2:385–390
26. Aatiq A, Menetrier M, Croguennec L et al (2002) On the structure of $Li_3Ti_2(PO_4)_3$. J Mater Chem 12:2971–2978
27. Aono H, Sugimoto E, Sadaoka Y et al (1991) Electrical property and sinterability of $LiTi_2(PO_4)_3$ mixed with lithium salt (Li_3PO_4 or Li_3BO_3). Solid State Ionics 47:257–264
28. Shimonishi Y, Zhang T, Imanishi N et al (2011) A study on lithium/air secondary batteries–stability of the NASICON-type lithium ion conducting solid electrolyte in alkaline aqueous solutions. J Power Sour 196:5128–5132
29. Robertson AD, West AR, Ritchie AG (1997) Review of crystalline lithium-ion conductors suitable for high temperature battery applications. Solid State Ionics 104:1–11
30. Kanno R, Hata T, Kawamoto Y, Irie M (2000) Synthesis of a new lithium ionic conductor, thio-LISICON lithium germanium sulfide system. Solid State Ionics 130:97–104
31. Murayama M, Kanno R, Kawamoto Y, Kamiyama T (2002) Structure of the thio-LISICON, Li_4GeS_4. Solid State Ionics 154–155:789–794
32. Murayama M, Kanno R, Irie M, Ito S, Hata T, No Sonoyama, Kawamoto Y (2002) Synthesis of new lithium ionic conductor Thio-LISICON—lithium silicon sulfides system. J Solid State Chem 168:140–148
33. Warburg E (1913) Über die Diffusion von Metallen in Glas. Ann Phys 40:327–334
34. Kunze D (1973) Silver ion conducting electrolyte with glass-like structure. In: Van Gool W (ed) Fast ion transport in solids. North Holland, Amsterdam, pp 405–408
35. Chiodelli G, Magistris A, Schiraldi A (1974) Some solid electrolyte cells. Electrochim Acta 19:655–656
36. Zachariasen WH (1932) The atomic arrangement in glass. J Am Chem Soc 54:3841–3851
37. Tomasi C, Mustarelli P, Magistris A (1998) Devitrification and metastability: revisiting the phase diagram of the system $AgI:Ag_2MoO_4$. J Solid State Chem 140:91–96
38. Barney ER, Hannon AC, Holland D, Winslow D, Rjial B, Affatigato M, Feller SA (2007) Structural studies of lead aluminate glasses. J Non-Cryst Solids 353:1741–1747
39. Mustarelli P, Quartarone E, Benevelli F (1997) A ^{11}B and ^{7}Li MAS-NMR study of sol-gel lithium triborate glass subjected to thermal densification. Mat Res Bull 32:679–687
40. Hayashi A, Hama S, Morimoto H et al (2001) Preparation of Li2S-P2S5 amorphous solid electrolytes by mechanical milling. J Am Ceram Soc 84:477–479
41. Anderson OL, Stuart DA (1954) Calculation of activation energy of ionic conductivity in silica glasses by classical methods. J Am Ceram Soc 37:573–780
42. Martin SW (1988) Conductivity activation energy relations in high sodium-content borate and aluminoborate glasses. J Am Ceram Soc 71:438–445
43. Ravaine D, Souquet JL (1977) A thermodynamic approach to ionic conductivity in oxide glasses. Part. 1. Correlation of the ionic conductivity with the chemical potential of constituents in binary alkali oxide glasses. Phys Chem Glasses 18:27–31
44. Ravaine D, Souquet JL (1978) A thermodynamic approach to ionic conductivity in oxide glasses. Part. 2. A statistical model for the variations of the chemical potential of constituents in binary alkali oxide glasses. Phys Chem Glasses 19:115–120
45. Martin SW, Angell CA (1986) Dc and ac conductivity in wide composition range Li2O-P_2O_5 glasses. J Non-Cryst Solids 83:185–207
46. Haven Y, Verkerk B (1965) Diffusion and electrical conductivity of sodium ions in sodium silicate glasses. Phys Chem Glasses 6:38–45
47. Charles RJ (1961) Polarization and diffusion in silicate glasses. J Appl Phys 32:1115–1126
48. Moynihan CT, Lesikar AV (1981) Weak-electrolyte models for the mixed alkali effectin glass. J Am Ceram Soc 64:40–46
49. Nassau K, Glass AM, Grasso M et al (1981) Quenched lithium-containing multiple sulphate glasses. J Non-Cryst Solids 46:45–58
50. Angell CA (1986) Recent developments in fast ion transport in glassy and amorphous materials. Solid State Ionics 18&19:72–88

51. Kawamura J, Shimoji M (1986) Ionic conductivity and glass transition in superionic conducting glasses $(AgI)_{1-x}(Ag_2MoO_4)_x$ (x = 0.25, 0.30, 0.35): I. Experimental results in the liquid and glassy states. J Non-Cryst Solids 88:281–294
52. Ingram MD, Mackenzie MA, Muller W et al (1988) Cluster and pathways: a new approach to ion migration in glass. Solid State Ionics 28–30:677–680
53. Senapati H, Parthasarathy G, Lakshmikumar SK et al (1983) Effect of pressure on the fast-ion conduction in silver iodide-silver oxide-molybdenum oxide glasses. Phil Mag B 47:291–297
54. Bunde A, Ingram MD, Maass P et al (1991) Mixed alkali effects in ionic conductors: a new model and computer simulations. J Non-Cryst Solids 131:1109–1112
55. Maass P, Bunde A, Ingram MD (1992) Ion transport anomalies in glasses. Phys Rev Lett 68:3064–3067
56. Funke K, Banhatti RD, Radha D (2006) Ionic motion in materials with disordered structures. Solid State Ionics 177:1551–1557
57. Mustarelli P, Tomasi C, Magistris A (2005) Fractal nanochannels as the basis of the ionic transport in AgI-based glasses. J Phys Chem B 109:17417–17421
58. St Adams, Swenson J (2000) Determining ionic conductivity from structural models of fast ionic conductors. Phys Rev Lett 84:4144–4147
59. Button DP, Tandon RP, Tuller HL et al (1981) Fast Li^+ conductance in chloroborate glasses II-diborates and metaborates. Solid State Ionics 5:655–658
60. Magistris A, Chiodelli G, Villa M (1985) Lithium borophosphate vitreous electrolytes. J Power Sour 14:87–91
61. Desphande V, Pradel A, Ribes M (1988) The mixed glass former effect in the Li_2S:SiS_2:GeS system. Mat Res Bull 23:379–384
62. Yamauchi A, Sakuda A, Hayashi A, Tatsumisago M (2013) Preparation and ionic conductivities of $(100 - x)(0.75Li_2S{:}0.25P_2S_5){:}x LiBH_4$ glass electrolytes. J Power Sour 244:707–710
63. Seino Y, Ota T, Takada K, Hayashi A, Tatsumisago M (2014) A sulphide lithium superion conductor is superior to liquid ion conductors for use in rechargeable batteries. Energy Environ Sci 7:627–631
64. Maranas JK (2012) Polyelectrolytes for batteries: current state of understanding. In Page K (ed) Polymers for energy storage and delivery: polyelectrolytes and fuel cells. ACS Symposium Series. American Chemical Society, Washington
65. Armand M, Chabagno JM, Duclot MJ (1979). In: Vashishta P (ed) Fast ion transport in solids. North Holland, New York
66. Gray FM (1997) Polymer electrolytes. Roy Soc Chem, London
67. Arora P, Zhang Z (2004) Battery separators. Chem Rev 104:4419–4462
68. Armand MB, Bruce PG, Forsyth M et al (2011) Polymer electrolytes in energy materials. In: Bruce DW, O'Hare D, Walton RI (eds) Wiley, Chichester
69. Hollinan DT, Balsara NP (2013) Polymer electrolytes. Annu Rev Mater Res 43:503–525
70. Ratner MA, Shriver DF (1988) Ion transport in solvent-free polymers. Chem Rev 88:109–124
71. Christie AM, Lilley SJ, Staunton E et al (2005) Increasing the conductivity of crystalline polymer electrolytes. Nature 433:50–53
72. Mazor H, Golodnitsky D, Peled E et al (2008) A search for single-ion conducting polymer electrolyte: combined effect of anion trap and inorganic filler. J Power Sour 178:736–743
73. Quartarone E, Mustarelli P (2014) Polyelectrolytes for batteries, encyclopedia of polymeric nanomaterials. Springer, Berlin, pp 1–10
74. Gomez ED, Panday A, Feng EH et al (2009) Effect of ion distribution on conductivity of block copolymer electrolytes. Nano Lett 9:1212–1216
75. Quartarone E, Mustarelli P, Magistris A (1998) PEO-based composite electrolytes. Solid State Ionics 110:1–14
76. Ohno H (2007) Design of ion conductive polymers based on ionic liquids. Macromol Symp 249–250:551–556
77. Mecerreyes D (2011) Polymeric ionic liquids: broadening the properties and applications of polyelectrolytes. Progr Pol Sci 36:1629–1648

78. Fourquet JL, Duroy H, Crosnier-Lopez MP (1996) Structural and microstructural studies of the series $La_{2/3-x}Li_{3x}\square_{1/3-2x}TiO_3$. J Solid State Chem 127:283–294
79. Inaguma Y, Katsumata T, Itoh M et al (2002) Crystal structure of a lithium ion-conducting perovskite $La_{2/3-x}Li_{3x}TiO_3$ (x = 0.05). J Solid State Chem 166:67–72
80. Tiyapiboonchaiya C, Pringle JM, Sun J et al (2004) The zwitterion effect in high-conductivity polyelectrolytes materials. Nat Mater 3:29–32